Interaction of dark solitons with localized impurities in Bose-Einstein condensates

Dimitri J. Frantzeskakis,[1] G. Theocharis,[1] F. K. Diakonos,[1] Peter Schmelcher,[2] and Yuri S. Kivshar[3]
[1]*Department of Physics, University of Athens, Panepistimiopolis, Zografos, Athens 15784, Greece*
[2]*Theoretische Chemie, Physikalisch-Chemisches Institut, INF 229, 69120 Heidelberg, Germany*
[3]*Nonlinear Physics Group, Research School of Physical Sciences and Engineering, Australian National University, Canberra ACT 0200, Australia*
(Received 28 June 2002; published 12 November 2002)

We study the interaction of dark solitons with a localized impurity in Bose-Einstein condensates. We apply the soliton perturbation theory developed earlier in optics for describing the soliton dynamics and soliton-impurity interaction analytically, and then verify the results by direct numerical simulations of the Gross-Pitaevskii equation. We find that a dark soliton can be reflected from or transmitted through a repulsive impurity in a controllable manner, while near the critical point the soliton can be quasitrapped by the impurity. Additionally, we demonstrate that an immobile soliton may be captured and dragged by an adiabatically moving attractive impurity.

DOI: 10.1103/PhysRevA.66.053608 PACS number(s): 03.75.Fi, 05.45.Yv, 05.30.Jp, 02.30.Jr

I. INTRODUCTION

Since the experimental discovery of Bose-Einstein condensation in dilute atomic alkali-metal gases [1] an enormous development of our knowledge on the properties of the condensed phase has taken place. Among others, experiments on the Bose-Einstein condensates (BECs) have demonstrated superfluidity of the condensed phase [2], the possibility of four-wave mixing [3], the amplification of light and atoms via a condensate [4] as well as the creation of topological structures such as vortices [5], vortex lattices [6], as well as dark [7] and bright [8] solitons. This opens the promising perspective for numerous applications of the nonlinear matter-wave physics and, in particular, it is very much reminiscent of the situation encountered for light waves and optics many decades ago. One of the first and recently invented example of a coherent matter-wave device is the so-called atom chip [9], that consists of a microfabricated semiconductor surface accommodating atom-optics elements such as current or charge-carrying wires, resonators, etc. The latter allow to trap and guide or, more generally speaking, to control the motion of the matter waves. A long-term perspective of such coherent matter-wave devices is quantum information processing on the nanometer scale.

A relevant interesting issue in the above context is to learn how to control the motion of nonlinear excitations of the condensate, in general, and of different types of solitons, in particular. Experimentally there exist several quantum-phase-engineering techniques to generate dark solitons in a Bose-Einstein condensate (see, e.g., Denschlag *et al.* [7]). The question then arises how one could influence or even guide their motion. The present paper makes a step in this direction by investigating the interaction of a dark soliton trapped in a confining potential with a localized inhomogeneity or an impurity. The perspective hereby is that impurities could be used as elements of a matter-wave device that controls the motion of a network of nonlinear excitations.

Dark solitons can be excited in BECs with repulsive interactions; such a soliton is characterized by a notch in the BEC density profile and a phase jump across its localized region. Their dynamics in a trapping potential has been studied theoretically by several authors [10–13]. Beyond the above motivation, the dynamics of BECs in the presence of impurities has recently become a subject of growing interest [14]. One process that has been studied is a response of the condensate to the propagation of significantly heavier impurities. The travelling impurity induces a BEC dynamics that leads, due to energy reasons, to the expulsion of the impurity from BEC. In this context, the investigation of the interaction of a soliton with a single impurity appears to be an important issue. It is of fundamental interest in nonlinear wave theory and has been studied in the framework of almost all nonlinear evolution equations possessing soliton solutions [15]. However, in the context of BECs where the relevant evolution equation is the Gross-Pitaevskii (GP) equation with a confining potential [16], the interaction of dark solitons with impurities has not been studied in detail yet.

The purpose of this paper is twofold. First, we apply the soliton perturbation theory earlier developed for dark solitons in optics (see Ref. [17] for a comprehensive review) and derive an effective equation for the motion of a dark soliton in a trapping potential, and in the presence of either repulsive or attractive impurities. Second, we study, both analytically and numerically, the dynamics of the condensate and a dark soliton in the presence of a static (nonpropagating) impurity. This analysis is rather general, and it may be used to describe the interaction of a dark soliton with ''artificial'' impurities induced by sharply focused laser beams used to engineer the density of the BEC in experiments [7]. Various interaction effects such as reflection, transmission, and quasitrapping of the dark soliton by a repulsive impurity are described and verified by direct simulations. The quasitrapping effect found is characterized by a relatively large time for the soliton-impurity interaction, and is followed by subsequent soliton oscillation in a limited spatial domain. Additionally, the possibility of the dragging of a dark soliton by an adiabatically moving attractive impurity is demonstrated.

The paper is organized as follows. In Sec. II, we describe our analytical results based on the perturbation theory invented for optical dark solitons. Section III is devoted to a

detailed comparison between our analytical predictions and numerical results obtained by the direct integration of the GP equation. Finally, Sec. IV provides a summary and conclusions.

II. MODEL AND ANALYTICAL RESULTS

A. The effective Thomas-Fermi wave function

A convenient model to study the mean-field dynamics of BECs is the GP equation which has the form of a $(3+1)$-dimensional nonlinear Schrödinger (NLS) equation with an external trapping potential (see, e.g., a review paper [16], and references therein). In the case when the confinement for two of the three spatial dimensions is much stronger than in the third dimension, the GP equation can be reduced to an effective quasi-$(1+1)$-dimensional GP equation [18] (see also the relevant experimental works in Refs. [7,19]). For repulsive interatomic interactions, the latter equation can be expressed in the following dimensionless form:

$$iu_t + \frac{1}{2}u_{xx} - |u|^2 u = V(x)u, \tag{1}$$

where the spatial coordinate x and time t are normalized to the harmonic-oscillator length $\alpha_\perp = \sqrt{\hbar/m\omega_\perp}$ and oscillation period, $1/\omega_\perp$, respectively. The frequency $\omega_\perp$ belongs to the two dimensions with strong confinement. The normalized field u describes the macroscopic wave function ψ of the condensate, according to the following scaling relation:

$$\psi(x,t) = \left(\frac{m\omega_\perp}{4\pi\alpha\hbar}\right)^{1/2} u(x,t),$$

where α is the scattering length.

In order to study the interaction of a BEC dark soliton with a localized impurity in the framework of Eq. (1), it is convenient to decompose the external potential $V(x)$ as follows:

$$V(x) = U_{\rm tr}(x) + b\,\delta(x), \tag{2}$$

where $U_{tr}(x)$ is the (conventional parabolic) time-independent trapping potential, which is assumed to be smooth and slowly varying on the soliton scale, and the additional sharp potential $\delta(x)$ accounts for an impurity localized in space at the point $x=0$, and it is described by a Dirac δ function. The parameter b in Eq. (2) which measures the impurity strength is assumed to be small and may take either positive or negative values for repulsive or attractive impurities, respectively. The impurity potential causes a deformation of the condensate wave function [14].

In order to treat analytically Eq. (1), first we look for the profile of the background field oscillations, $u = u_b(x)e^{-iu_0^2 t}$, where u_0^2 is the normalized density of the BEC cloud, in the presence of the potential $V(x)$ that is given by the real equation

$$u_0^2 u_b + \frac{1}{2}\frac{d^2u_b}{dx^2} - u_b^3 = V(x)u_b\,. \tag{3}$$

When the amplitude $\max|u_b(x)|$ is small, the nonlinear term in Eq. (3) can be neglected and, assuming that in the absence of the potential $V(x)$ the background amplitude is u_0, we look for a solution of Eq. (3) in the form

$$u_b(x) = u_0 + f(x). \tag{4}$$

Substituting Eq. (4) into Eq. (3), neglecting all nonlinear terms with respect to f and keeping only the leading-order terms with respect to the parameters b and k (see below), we obtain the following linear equation for $f(x)$:

$$\frac{1}{2}\frac{d^2f}{dx^2} - 2u_0^2 f = u_0[U_{\rm tr}(x) + b\,\delta(x)]. \tag{5}$$

A physically relevant solution of Eq. (5) may be obtained as follows: First, in the absence of the impurity (i.e., in the case $b=0$), we assume an anisotropic cigar-shaped harmonic trap, described by the effective one-dimensional potential $U_{\rm tr}(x) = k^2x^2$, where $k^2 = (\omega_x^2/2\omega_\perp^2) \ll 1$, ω_x being the frequency of the trap in the axial direction. In this case, the spatial derivative d^2f/dx^2 is small and can be neglected, and, as a result, an approximate solution of Eq. (5) reads $f(x) = -(2u_0)^{-1}U_{\rm tr}(x)$, resembling the well-known Thomas-Fermi (TF) approximation for the wave function, where the density $|u|^2$ is quadratic in the term $u_0 - U_{\rm tr}(x)$. Second, for a homogeneous BEC (i.e., in the case $U_{\rm tr}=0$), Eq. (5) is equivalent to its homogeneous counterpart and the matching condition at the position of the impurity reads

$$\left.\frac{df}{dx}\right|_{0_+} - \left.\frac{df}{dx}\right|_{0_-} = 2bu_0\,.$$

Therefore, the spatially localized solution of Eq. (5) is $f(x) = -(b/2)\exp(-2u_0|x|)$. Combining these particular solutions, we express the solution of Eq. (5) as follows:

$$f(x) = -\frac{1}{2u_0}U_{\rm tr}(x) - \frac{b}{2}e^{-2u_0|x|}. \tag{6}$$

The background field density $u_b^2(x)$ given by Eqs. (4) and (6) actually describes an effective TF-like condensate wave function modified by a localized impurity. This density is illustrated in Fig. 1 (solid line) for $u_0=1$ and for the harmonic trapping potential $U_{\rm tr}(x) = (kx)^2$ (dashed line), with $k=0.05$; this value is approximately twice as large the one used in the experimental studies of BEC dark solitons in Ref. [7]. We remark that both for the illustrations [see Fig. 1] as well as the numerical calculations the δ function for the localized impurity at $x=0$ has been replaced by the steep function $10b\cosh^{-1}(x/0.05)$ with $b=\pm 0.15$ for repulsive or attractive impurities, respectively. It is interesting to observe that the repulsive impurity [Fig. 1(a)] creates a hole on the condensate wave function, in accordance with the earlier predictions [14], while the attractive one [Fig. 1(b)] creates a hump. In any case, it is clear that the condensate is shaped like the inverted harmonic trapping potential with a dip or a hump, having the size of the healing length (which is,

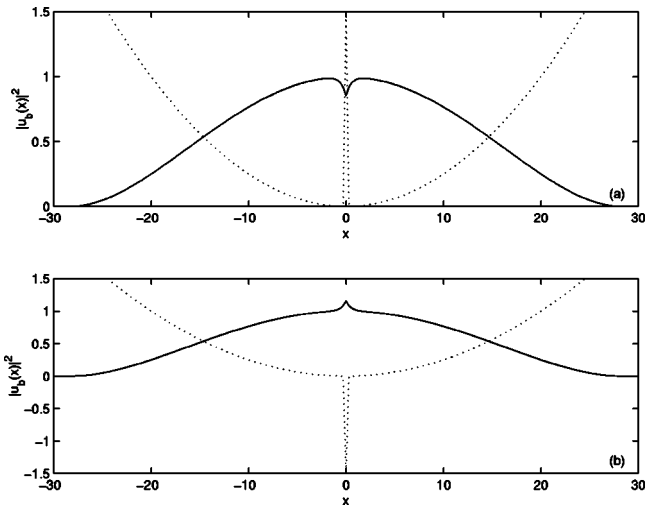

FIG. 1. The ground-state condensate intensity $u_b^2(x)$ (solid), describing an effective Thomas-Fermi cloud, for a harmonic trapping potential $U_{\rm tr}(x)=(kx)^2$ (dotted) with $k=0.05$. The potential due to the localized impurity at $x=0$ is approximated by the steep function $10b\ \cosh^{-2}(x/0.05)$ with $b=\pm 0.15$. Both cases of repulsive (a) and attractive (b) impurities are, respectively, shown.

roughly speaking, equal to 1/56 for the values of the parameters used) around the impurity.

B. Dynamics of dark solitons

To describe the dynamics of a dark soliton on top of the inhomogeneous background described by the effective TF-like cloud, we seek for a solution of Eq. (1) in the form

$$u=u_b(x)e^{-iu_0^2t}v(x,t), \tag{7}$$

where u_b obeys Eq. (3) and the unknown complex field $v(x,t)$ represents a dark soliton, which is governed by the following effective equation:

$$iv_t+\frac{1}{2}v_{xx}-u_b^2(|v|^2-1)v=-\frac{1}{u_b}\frac{du_b}{dx}v_x. \tag{8}$$

Apparently, the right-hand side and part of the nonlinear terms of Eq. (8) can be treated as a perturbation. To obtain the contribution of the nonlinear terms within perturbation theory, we may use Eqs. (4) and (6) and approximate u_b^2 as $u_b^2\approx u_0^2+2u_0f$, based on the smallness of the function $f(x)$ (due to the slowly varying properties of the trapping potential and the smallness of the parameter b characterizing the impurity). In this way, and upon introducing the transformations $t\to u_0^2t$, $x\to u_0x$, we obtain the following perturbed NLS equation for the dark soliton:

$$iv_t+\frac{1}{2}v_{xx}-(|v|^2-1)v=P(v), \tag{9}$$

where the total perturbation $P(v)$ has the form

$$P(v)=\frac{1}{2u_0^2}\left[2(1-|v|^2)vU_{\rm tr}+v_x\frac{dU_{\rm tr}}{dx}\right]+\frac{b}{u_0}e^{-2u_0|x|}[(1-|v|^2)v-u_0(x/|x|)v_x]. \tag{10}$$

In the absence of the perturbation $P(v)$, Eq. (9) represents a conventional defocusing NLS equation which has a dark soliton solution of the form [22]

$$v(x,t)=\cos\varphi\tanh\xi+i\sin\varphi,\quad \xi=\cos\varphi[x-(\sin\varphi)t], \tag{11}$$

where φ is the soliton phase angle ($|\varphi|<\pi/2$) describing the *darkness* of the soliton through the relation, $|v|^2=1-\cos^2\varphi/\cosh^2\xi$ (note that the limiting cases $\varphi=0$ and $\cos\varphi\ll 1$ correspond to the so-called *black* and *gray* solitons, respectively [17]). To treat analytically the effect of the perturbation (10) on the dark soliton, we employ the adiabatic perturbation theory developed in Ref. [20] (see also the review [17]). According to this approach, the parameters of the dark soliton (11) become slowly varying functions of t, but the functional form remains unchanged. Thus, the soliton "phase angle" becomes $\varphi\to\varphi(t)$ and, as a result, the soliton coordinate becomes $\xi\to\xi=\cos\varphi(t)[x-x_0(t)]$, where

$$x_0(t)=\int_0^t\sin\varphi(t')dt' \tag{12}$$

is the soliton center. As has been shown in Ref. [20], the evolution of the parameter φ is then defined by the equation,

$$\frac{d\varphi}{dt}=\frac{1}{2\cos^2\varphi\sin\varphi}\,{\rm Re}\left\{\int_{-\infty}^{+\infty}P(v)v_t^*dx\right\}. \tag{13}$$

Substituting Eq. (10) into Eq. (13) and taking into account that for spatially slowly varying trapping potential $U_{\rm tr}$ the higher-order derivatives may be omitted, we obtain the following result (for $u_0=1$):

$$\frac{d\varphi}{dt}=-\frac{1}{2}\frac{dU_{\rm tr}}{dx}+\frac{3}{4}b\int_0^{+\infty}dx\frac{\exp(-2x)}{[\cosh^4(x-x_0)-\cosh^4(x+x_0)]}, \tag{14}$$

where we assume additionally that the dark soliton is close to a black one, i.e., φ is sufficiently small. Evaluating the integrals in Eq. (14) and using the definition of Eq. (12), we obtain the following effective equation for the soliton center:

$$\frac{d^2x_0}{dt^2}=-\frac{dW}{dx_0}. \tag{15}$$

It is readily seen that Eq. (15) represents an equation of motion for a classical particle with the coordinate x_0 moving in the effective potential,

$$W(x_0)=\frac{1}{2}\left\{U_{\rm tr}(x_0)+\frac{b}{2\cosh^2 x_0}\right\}. \qquad (16)$$

It is important to notice that, in the absence of the impurity ($b=0$), Eq. (15) describes the motion of a dark soliton in the presence of a trapping potential, and it predicts that the soliton oscillates in a harmonic trap. An equation similar to Eqs. (15), (16) has first been stated without derivation in Ref. [10], but without the factor of 1/2. The same equation found in Ref. [10] is derived in Ref. [11] by considering the dipole mode of a condensate carrying a dark soliton, and thus it is not directly related to Eq. (15). The correct result has been obtained by a multiple time scale boundary layer theory recently developed by Busch and Anglin [12] who assumed that the potential, the background density, and velocity vary slowly on the soliton scale.

In the general case $b\neq 0$, we do not assume that the impurity potential varies slow on the soliton scale, however, we take into account the modification of the condensate ground state in the presence of the impurity. It is important to mention that the term proportional to b in the potential (16) does not possess the appearance one might expect by inspecting Eqs. (5) and (6). This reflects the pointlike character of the impurity: the healing length is the shortest length available in the condensate with respect to density variations and the effective pointlike impurity generates a disturbance of the background cloud on the same length scale as the dark soliton.

The resulting equation (16) shows that the character of the effective potential is changed in the vicinity of the impurity (i.e., in a localized region around $x=0$): In particular, it becomes repulsive (attractive) for $b>0$ ($b<0$) for the dark soliton due to the presence of the impurity localized at the center of the trapping potential.

III. NUMERICAL RESULTS

Adopting the particle picture of the dark soliton described above, we now analyze the soliton dynamics in the framework of Eqs. (15) and (16). In particular, we assume that the effective potential is given by $W(x_0)=(1/2)(kx_0)^2+(b/4)\cosh^{-2}(x_0)$ (the values of the parameters are $k=0.05$ and $b=\pm 0.15$, see Fig. 1).

At first, in the case of a repulsive impurity ($b>0$) [see $W(x_o)$ in Fig. 2(a)], it is clear that the dynamical system in hand is characterized by three fixed points, namely, two elliptic (stable) located at $x_0\approx\pm 2$ and one hyperbolic (unstable) located at $x_0=0$. Figure 2(b) shows the associated phase plane $(x_0, dx_0/dt)$ including several phase curves. The separatrix passing through the hyperbolic fixed point at (0,0) possesses the appearance of an intersecting double loop and, by definition, separates two types of motion taking place in a single well or above both wells. As a result, different types of the soliton dynamics and soliton-impurity interaction are expected, depending on the initial conditions [recall that we consider almost black solitons with $\cos\varphi\approx 1$, i.e., the initial soliton velocity is $\sin\varphi\approx 0$, and, as a result, the initial conditions refer solely to the initial soliton position $x_0(0)$]:

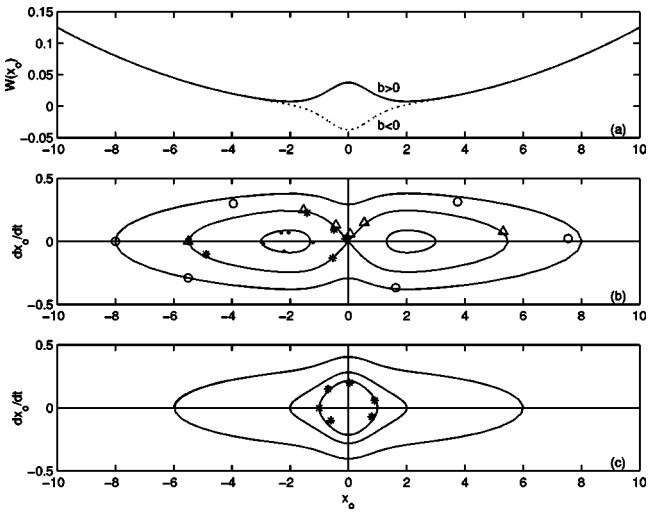

FIG. 2. (a) The effective potential $W(x_0)=(1/2)(0.05x_0)^2+(b/4)\cosh^{-2}(x_0)$ for a repulsive impurity, $b=0.15$ (solid line), and an attractive impurity, $b=-0.15$ (dotted line). (b) The associated phase plane for $b=+0.15$, where several trajectories are shown. Dots, small circles, diamonds, and stars correspond to the numerical results obtained by direct integration of the GP equation for different initial positions of the soliton taken inside, outside, or on the left-hand separatrix, respectively. The corresponding types of the soliton dynamics are shown in Figs. 3, 4, 5, and 6, respectively. (c) The associated phase plane for $b=-0.15$, where several trajectories are shown. Stars correspond to the numerical results obtained by the GP equation for $t=0,5,8,15,20,30$, for a black soliton initially placed at $x_0=-1$.

(a) For $|x_0(0)|<5.48$ (corresponding to the phase curves surrounding the elliptic fixed points) the dark soliton is *reflected* nearly elastically by the impurity, and then it oscillates in a relatively small spatial region [see Fig. 1(b)], as compared to the entire length of the condensate (the latter is $L\approx 56$).

(b) For $|x_0(0)|>5.48$ (corresponding to the phase curves surrounding the separatrix) the dark soliton is *transmitted* nearly elastically through the impurity, and then it oscillates in a relatively large region in x, as compared to the entire length of the condensate.

(c) The point $|x_0(0)|=5.48$ corresponds to a critical regime described by the figure-eight separatrix; in this case the interaction time is very large.

On the other hand, in the case of an attractive impurity ($b<0$), as shown in Fig. 2(a), it is clear that the dynamical system in hand is characterized by a single fixed point, namely, an elliptic (stable) one, located at $x_0=0$. Figure 2(c) shows the associated phase plane including several phase curves. Apparently all trajectories are periodic and the spatial domain where the soliton oscillates is the same as in the case $b=0$. Thus, the presence of the attractive impurity does not qualitatively affect the soliton motion, but rather modifies locally (i.e., in the vicinity of the site of the impurity) the soliton's kinetic energy.

The above theoretical predictions have been checked by direct numerical simulations of the GP equation. In particular, we have used a split-step Fourier method [21] to inte-

grate the GP equation (1) with an initial condition of the form

$$u(x,0)=u_b(x)\tanh[x-x_0(0)], \tag{17}$$

where $u_b(x)=1+f(x)$ is the effective TF-like wave function modified by the localized impurity [$f(x)$ is given in Eq. (6) with $u_0=1$] and $x_0(0)$ is the initial soliton position. This initial condition represents a dark soliton with $\cos\varphi=1$ [see Eq. (11)], i.e., a black soliton with zero initial velocity. Notice that the particular choice of the initial condition (17) implies that the characteristic length k^{-1} of the trapping potential is much larger than the soliton width, i.e., $k^{-1}\gg 1$ (recall that we have taken $k=0.05$), a fact indicating that in this regime the validity of the perturbation theory presented in the preceding section is guaranteed.

Finally, it is important to notice that since the initial condition used [see Eq. (17)], is obviously only an approximation and not an exact solution of the GP equation with the impurity, it does not describe the pure soliton state, but also includes various phonon modes. Consequently, in the numerical results presented below, changes in the background density of the condensate, even ''far'' away from the soliton, are observed. Also in an experiment, the prepared soliton does not perfectly coincide with the theoretical analytically or numerically obtained soliton. We expect that our analytical predictions and numerical results (which, as we will see below, are in a fairly good agreement) can be verified in a corresponding experiment.

A. Repulsive impurity

The three different types (a), (b), and (c) of the soliton evolution and interaction with a repulsive impurity predicted above, have been investigated numerically upon considering the initial soliton positions $x_0(0)=-3$, -8, -5.48, and -5.5, respectively.

In particular, Fig. 3 shows the evolution of the soliton density $|u|^2$, corresponding to Eq. (17) with $x_0(0)=-3$, on top of the effective TF cloud (solid line), with a potential $V(x)=(0.05x)^2+1.5\cosh^{-2}(x/0.05)$ (dotted line). Notice that both the effective TF wave function and potential are the same as the ones illustrated in Fig. 1(a). As can be seen in Fig. 3, the dark soliton is reflected by the impurity (at $t\approx 28$; see third panel) nearly elastically, and it oscillates in the interval $-3<x<-1$. The oscillations of the soliton take place in a spatial domain significantly smaller than the extension of the BEC trap (here the corresponding fraction is 2/56). According to the particle picture of the soliton adopted in the preceding section, this behavior is effectively described by a periodic trajectory inside the separatrix loop on the left-hand side of Fig. 2(b). To illustrate this, the numerically obtained soliton positions and velocities $(x_0,\ dx_0/dt)$ corresponding to the instants of the six subfigures of Fig. 3 are shown by six dots in Fig. 2(b), starting from $(-3,0)$ and taking place clockwise. It is clearly seen that the relevant analytical prediction, according to which the soliton center follows the periodic trajectory is in fairly good agreement with the numerical result obtained by the direct integration of the GP equation. This agreement is not only qualitative but quantitative, since the maximum relative error found in the soliton velocity does not exceed 20%.

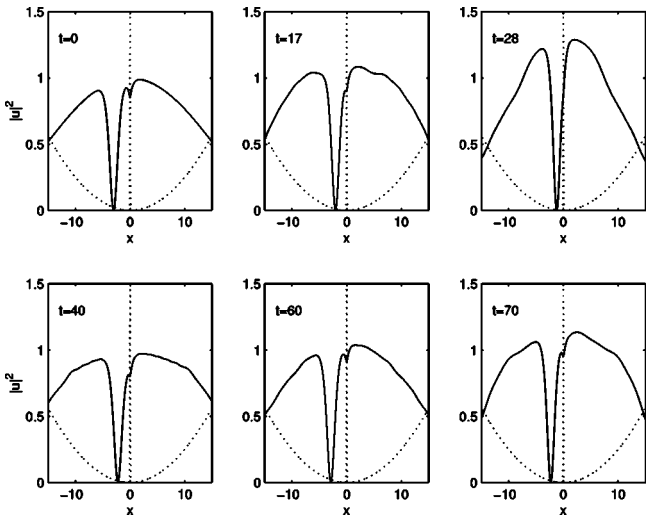

FIG. 3. Evolution of a black soliton density $|u|^2$ on top of the effective TF cloud (solid), with the potential $V(x)$ (dotted) being the same as the one in Fig. 1(a). The dark soliton is initially placed at $x_0(0)=-3$ and, in accordance with the analytical prediction, it is reflected by the impurity (at $t\approx 28$) and then oscillates in the interval $-3<x<-1$. This behavior is effectively described by the periodic trajectory surrounded by the left part of the separatrix shown in Fig. 2(b).

Using the same initial configuration for a dark soliton initially placed at $x_0(0)=-8$, in Fig. 4 we show the evolution of the soliton density which, in this case, is transmitted nearly elastically through the impurity (no emission of radiation is observed), i.e., it is oscillating in the interval $-8<x<7.5$. Thus, the soliton motion takes place in a relatively large spatial region compared to the condensate length (here

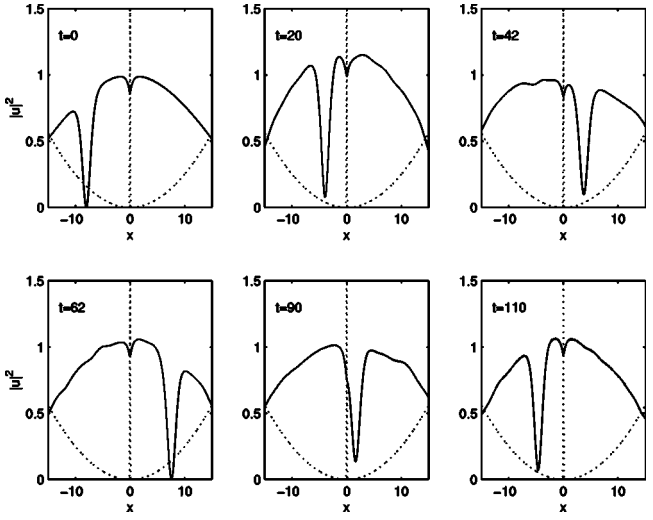

FIG. 4. The same as in Fig. 3 but for the dark soliton initially placed at $x_0(0)=-8$. According to the analytical results, the soliton is transmitted through the impurity and then oscillates in the interval $-8<x<7.5$. This behavior is effectively described by the periodic trajectory enclosing the separatrix in Fig. 2(b).

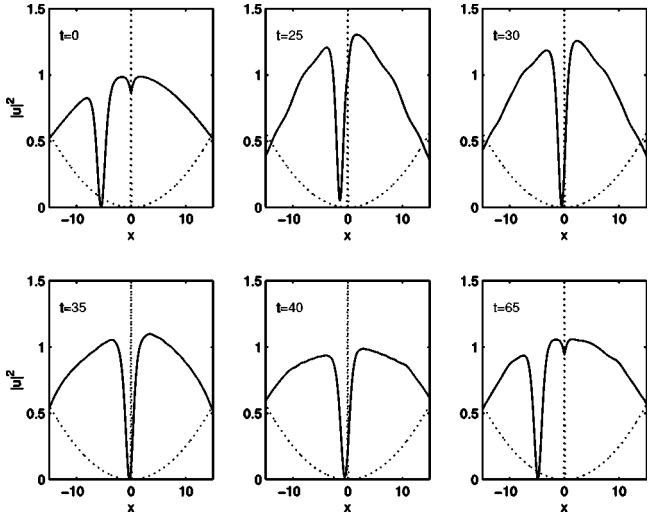

FIG. 5. The same as in Fig. 3 but for the dark soliton initially placed at $x_0(0)=-5.48$. The soliton reaches the point $x=0$, then it is quasitrapped by the impurity for some finite time, and eventually oscillates following a periodic trajectory enclosed by the left part of the separatrix in Fig. 2(b).

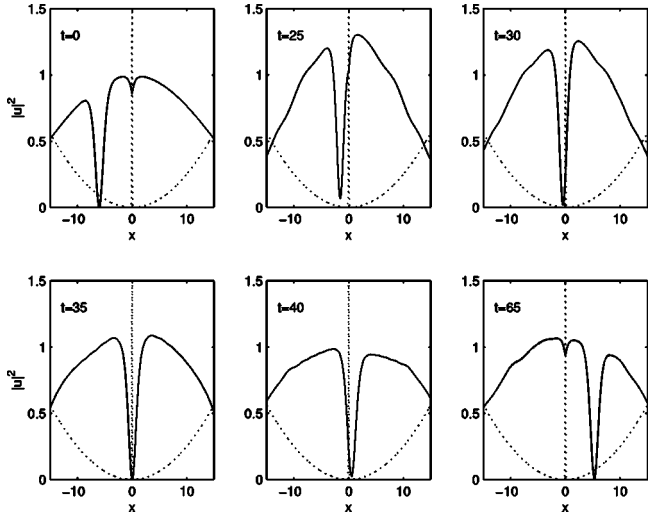

FIG. 6. The same as in Fig. 3 but for the dark soliton initially placed at $x_0(0)=-5.5$. The soliton reaches the point $x=0$, then it is quasitrapped by the impurity for some finite time, and eventually oscillates following a periodic trajectory that encloses the right part of the separatrix in Fig. 2(b).

the fraction is $\approx 15.5/56$). This behavior is effectively described by the periodic trajectory enclosing the separatrix shown in Fig. 2(b). As done above the soliton's position in phase space corresponding to the instants of the six subfigures of Fig. 4 are indicated (small circles) in Fig. 2(b). They follow the corresponding periodic trajectory and a good agreement between the analytical prediction and the numerical results is found again (the maximum relative error in the soliton velocity is found to be slightly smaller in this case, i.e., of the order of 15%).

We will now investigate the third possible type of soliton-impurity interaction corresponding to a critical regime. In Fig. 5, we show the evolution of a dark soliton with an initial position corresponding to the extremal value $x_{\max}$ of the left-hand part of the separatrix in Fig. 2(b). According to the previous discussion, it is expected that the dark soliton will interact infinitely long with the impurity approaching the point $x=0$. As can be seen in Fig. 5, in direct simulations the dark soliton reaches the impurity site (at $t\approx 30$) and it remains ''quasitrapped'' by the impurity till $t\approx 38$. Nevertheless, the numerical simulations show that for $t>38$ the soliton is released by the impurity, i.e., the soliton center, instead of remaining on the separatrix, escapes to a periodic trajectory inside the separatrix and eventually performs an oscillation. This behavior can be seen in Fig. 2(b), where the first four of the soliton's phase space points (corresponding to the six subfigures of Fig. 5) are indicated by stars and follow the separatrix (the maximum relative error in the soliton velocity found does not exceed 10%), while the last two phase space points follow a periodic trajectory inside the separatrix.

A slightly different initial soliton position, but still close to the separatrix, i.e., $x_0(0)=-5.5$ (note: this value is slightly smaller than the extremal value $x_{\max}$) produced similar results for the soliton-impurity interaction, but instead it leads to the soliton traversal through the impurity. This result is illustrated in Fig. 6, where the dark soliton, after reaching the impurity (at $t\approx 30$) first is trapped until $t\approx 38$, as in the previous case. However, for $t>38$ the soliton escapes to a nearby periodic trajectory surrounding the separatrix, eventually performing an oscillation in a relatively large spatial domain. This behavior can also be seen in Fig. 2(b) indicated by triangles that follow the separatrix (the maximum relative error in the soliton velocity found does not exceed 10%), while the last two triangles follow a periodic trajectory surrounding the separatrix. It is worth mentioning that, in both cases mentioned above, the trapping time is estimated to be of order $t_{\rm tr}\approx 10$.

Generally speaking, the initial conditions located in the neighborhood of the separatrix lead to a quasitrapping phenomenon characterized by a relatively large time $t_{\rm tr}$ of interaction between the dark soliton and impurity. This phenomenon is followed by either reflection or transmission and eventual oscillation of the soliton. Apparently, quasitrapping cannot be understood quantitatively in terms of perturbation theory since the latter predicts that the soliton will remain infinitely long at the impurity. However, it is worth mentioning that the perturbation theory developed above is based on the particlelike properties of the dark soliton, and it does not take into account the radiation component of the field, which describes the wave properties of the soliton. We strongly surmise that the quasitrapping effect is a signature of the wave nature of the soliton excitation, but its detailed investigation is beyond the scope of this paper.

We have also carried out numerical simulations for nearly black solitons characterized by a small initial velocity (e.g., $\sin\phi\approx 0.1$); these results provide a qualitatively similar picture for both the soliton evolution and soliton-impurity interaction. This can be understood in terms of the presented analysis, since nearly black solitons follow the trajectories on the phase plane in the neighborhood of the corresponding ones followed by the black solitons. For example, an initially finite soliton velocity may result in a change of reflection

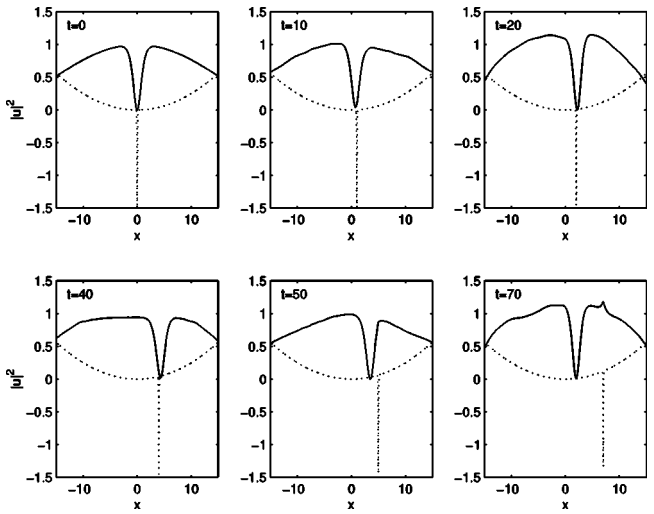

FIG. 7. Evolution of a black soliton density $|u|^2$ on top of the effective TF cloud (solid), with the potential $V(x)$ (dotted) being the same as that in Fig. 1(b). The dark soliton that is initially placed at $x_0(0)=0$ is captured and dragged by a steadily moving attractive ($b=-0.15$) impurity with a velocity $v=0.1$. This occurs up to $t \approx 40$, when the soliton is released by the impurity, and eventually oscillates following a periodic trajectory in the interval $-4 \leqslant x \leqslant 4$.

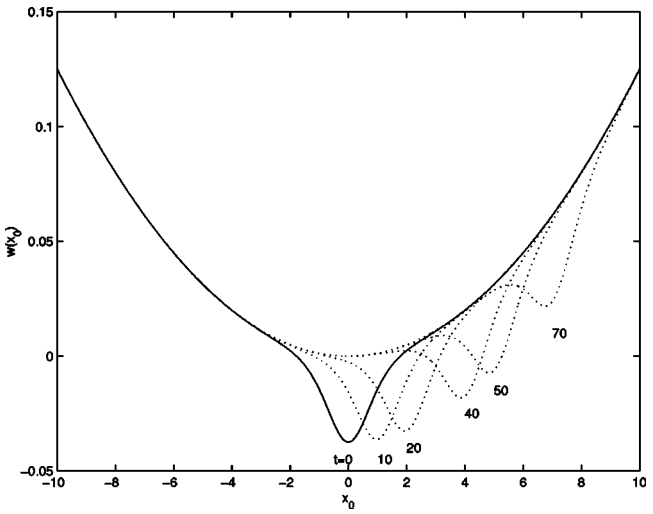

FIG. 8. The effective potential $W(x_0)$ in the case of a steadily moving attractive impurity with $b=-0.15$ and velocity $v=0.1$ for time instants corresponding to the snapshots of Fig. 7. For $t<40$ the soliton performs oscillations in the deepest part of the potential, thus being pulled by the impurity. At $t \approx 40$ the formation of an additional maximum is observed and the potential becomes shallower, allowing the soliton to gain energy. This effect may qualitatively explain the release of the soliton by the moving impurity for later times.

into transmission, which can easily be understood, since this change of the initial conditions drives the soliton (after interacting for some finite time with the impurity) to follow a periodic orbit enclosing the separatrix.

B. Attractive impurity

Here we investigate numerically the dynamics of a nearly black soliton in the presence of an attractive impurity ($b<0$). As discussed above, in this case the effective potential becomes attractive for the dark soliton in the vicinity of the impurity (i.e., at $x=0$) as shown in Fig. 2(a). However, if a dark (black) soliton is initially located far away from the impurity (i.e., for $|x_0|>2$), there is no way to be trapped since its initial potential energy (due to the trapping potential) is larger than the depth of the impurity-induced well. On the other hand, if $|x_0|<2$ the black soliton oscillates in the attractive impurity-induced well, occupying a comparatively small region around the location of the impurity. Both these results have been confirmed by direct numerical simulations of the GP equation. Particularly, the oscillation of a black soliton, initially placed at $x_0=-1,-2,-6$, is illustrated in the associated phase plane shown in Fig. 2(c) by the corresponding periodic trajectories (solid lines). Again, the numerically found soliton positions and velocities [see points depicted by stars in Fig. 2(c)] in the case of a black soliton with $x_0=-1$ (i.e., initially located inside the well induced by the impurity), are in a fairly good agreement with the analytical predictions.

In this context, an interesting issue is to consider an adiabatically moving attractive impurity, which moves with a small constant velocity v on top of the background TF wave function without inducing significant perturbations. In this case, the question arises whether this steadily moving impurity may drag a black soliton, which is stationary if it is initially placed at the bottom of the trapping potential ($x=0$), or it slightly oscillates in the well induced by a static attractive impurity. Apparently this issue is important for applications, since it would directly demonstrate the possibility of controlling the motion of black solitons in BECs, by means of artificial impurities induced by properly tuned, sharply focused laser beams.

In order to investigate this issue, we have integrated numerically the original GP equation with the modified potential $V(x;t)=(0.05x)^2-1.5\cosh^{-2}[(x-vt)/0.05]$ and with an initial condition $u(x,0)=u_b(x)\tanh(x)$, i.e., a black soliton initially placed at the location of the impurity. In the numerical simulations, varying the value of the velocity v of the impurity, we observed that for $v>v_c \approx 0.25$ the black soliton remains immobile and the moving impurity causes strong fluctuations in the condensate background wave function. On the other hand, when v is taken below v_c the soliton is able to follow the impurity for a finite time, inversely proportional to the value of v. Such a case is illustrated in Fig. 7, where the evolution of a black soliton, dragged by a steadily moving impurity with $v=0.1$, is shown. It is clearly seen that the soliton is captured and pulled by the impurity up to $t \approx 40$, but later on it escapes and, having gained energy, it starts to oscillate in the interval $(-4,4)$ (note that at $t=40$ the soliton center is placed at $x=4$). In order to get a qualitative insight into this effect, in Fig. 8 we show the successive forms of the relevant effective potential $W(x_0)$ for the time instants corresponding to the snapshots in Fig. 7.

For $t<40$ the potential is always purely attractive and the dark soliton gets trapped and is transported by the impurity, performing, at the same time, small oscillations inside the well. However, at approximately $t=40$ an additional maximum forms and the potential becomes shallower. This allows the soliton to gain enough energy for performing larger oscillations (ignoring the barrier that is going to be formed), finally leading to an escape of the soliton from the moving impurity.

IV. SUMMARY AND CONCLUSIONS

We have studied the interaction of a dark soliton with a localized impurity in Bose-Einstein condensates. This situation has been modeled by an external potential in the GP equation, which, apart from the conventional confining potential of the trap, incorporates an additional δ-like potential. The latter provides a phenomenological description of the presence of a sufficiently narrow impurity compared to the BEC's length. Experimentally, such an impurity could be realized by a correspondingly focussed laser beam intersecting the condensate. The impurity potential modifies the background Thomas-Fermi wave function by forcing a hole (hump) at the location of a repulsive (attractive) impurity. We have studied the dynamics of a dark soliton placed on top of the effective TF cloud employing the perturbation theory for dark solitons earlier developed in optics [20]. According to this approach, the soliton-impurity interaction is effectively described in terms of a collective variable, the soliton center.

In the case of a repulsive impurity, we have demonstrated that the soliton behaves like a classical particle in the presence of an effective double-well potential, whose central local maximum is induced by the presence of the impurity. As a result, the perturbation theory predicts, depending on the initial conditions, an elastic soliton reflection by the impurity, and nearly elastic transmission through the impurity, both cases being accompanied by soliton oscillations in the relevant spatial domains. The analytical predictions are then compared to the results of the direct numerical integration of the GP equation. We find that there is a fairly good agreement between the analytical and numerical results for the soliton reflection and transmission through the impurity. Near the critical regime we observe a quasitrapping phenomenon, characterized by a relatively large interaction time and subsequent reflection or transmission of the dark soliton.

The dynamics of a dark soliton in the presence of an attractive impurity has been studied as well. In this case, we have shown that the soliton motion is not qualitatively affected by the impurity, since the soliton oscillates in the same spatial domains as in the case of a purely harmonic confining potential. Nevertheless, we have demonstrated that a black soliton, initially placed at the bottom of the confining potential, can be captured and dragged by an adiabatically moving attractive impurity, up to a certain time inversely proportional to the dragging velocity. It is found that the impurity-induced convection of the soliton occurs for impurity velocities below a certain threshold. The release of the soliton by the impurity after finite time has qualitatively been explained by adopting the particle picture of the soliton and its motion in the relevant effective time-dependent potential.

The above results show that spatially fixed or adiabatically moving impurities represent an effective tool for manipulating the soliton motion in the condensates: qualitatively different processes can, to some extent, be controlled by, e.g., the coupling strength of the impurity. Higher dimensions than the effective one-dimensional situation considered here as well as further possible elements to control the motion of nonlinear excitations are relevant issues to be considered in future investigations.

ACKNOWLEDGMENTS

This work has been partially supported by the Special Research Account of the University of Athens. D.J.F. appreciates the hospitality of the Department of Theoretical Chemistry at the University of Heidelberg. Valuable discussions with H.E. Nistazakis (University of Athens) on numerical simulations and with J. Schmiedmayer on matter-wave optics are gratefully acknowledged. The work of Y.S.K. has been partially supported by the Australian Research Council.

[1] M. H. Anderson *et al.*, Science **269**, 198 (1995); K. B. Davis *et al.*, Phys. Rev. Lett. **75**, 3969 (1995); C. C. Bradley *et al.*, *ibid.* **75**, 1687 (1995).
[2] R. Onofrio *et al.*, Phys. Rev. Lett. **85**, 2228 (2000).
[3] L. Deng *et al.*, Nature (London) **398**, 218 (1999).
[4] S. Inouye *et al.*, Phys. Rev. Lett. **85**, 4225 (2000).
[5] M. R. Matthews *et al.*, Phys. Rev. Lett. **83**, 2498 (1999); K. W. Madison, F. Chevy, W. Wohlleben, and J. Dalibard, *ibid.* **84**, 806 (2000); S. Inouye *et al.*, *ibid.* **87**, 080402 (2001); A. L. Fetter and A. A. Svidzinsky, J. Phys.: Condens. Matter **13**, R135 (2001).
[6] J. R. Abo-Shaeer, C. Raman, and W. Ketterle, Phys. Rev. Lett. **88**, 070409 (2002).
[7] S. Burger *et al.*, Phys. Rev. Lett. **83**, 5198 (1999); J. Denschlag *et al.*, Science **287**, 97 (2000).
[8] K. E. Strecker *et al.*, Nature (London) **417**, 150 (2002); L. Khaykovich *et al.*, Science **296**, 1290 (2002).
[9] D. Müller *et al.*, Phys. Rev. Lett. **83**, 5194 (1999); N. H. Decker *et al.*, *ibid.* **84**, 1124 (2000); D. Müller *et al.*, Opt. Lett. **25**, 1382 (2000); D. Cassettari *et al.*, Phys. Rev. Lett. **85**, 5483 (2000); J. Reichel *et al.*, Appl. Phys. B: Lasers Opt. **72**, 81 (2001); R. Folman *et al.*, Phys. Rev. Lett. **84**, 4749 (2000); W. Hansel *et al.*, Nature (London) **413**, 498 (2001); R. Folman *et al.*, Adv. At. Mol. Phys. (to be published).
[10] W. P. Reinhardt and C. W. Clark, J. Phys. B **30**, L785 (1997).
[11] S. A. Morgan, R. J. Ballagh, and K. Burnett, Phys. Rev. A **55**, 4338 (1997).
[12] Th. Busch and J. R. Anglin, Phys. Rev. Lett. **84**, 2298 (2000).
[13] X.-J. Chen, J.-Q. Zhang, and H.-C. Wong, Phys. Lett. A **268**, 306 (2000); L. D. Carr, J. Brand, S. Burger, and A. Sanpera,

Phys. Rev. A **63**, 051601(R) (2001); S. Burger, L. D. Carr, P. Öhberg, K. Sengstock, and A. Sanpera, *ibid.* **65**, 043611 (2002).

[14] A. Gold and A. Ghazali, J. Phys.: Condens. Matter **11**, 2363 (1999); A. P. Chikkatur *et al.*, Phys. Rev. Lett. **85**, 483 (2000); S. A. Chin and H. A. Forbert, Phys. Lett. A **272**, 402 (2000); P. Capuzzi, E. S. Hernandez, and M. Barranco, Phys. Rev. A **62**, 023603 (2000); P. Giacconi, F. Maltoni, and R. Soldati, Phys. Lett. A **279**, 12 (2001); R. M. Cavalcanti, P. Giacconi, G. Pupilo, and R. Soldati, Phys. Rev. A **65**, 053606 (2002).

[15] Yu. S. Kivshar and B. A. Malomed, Rev. Mod. Phys. **61**, 763 (1989).

[16] F. Dalfovo, S. Giorgini, L. P. Pitaevskii, and S. Stringari, Rev. Mod. Phys. **71**, 463 (1999).

[17] Yu. S. Kivshar and B. Luther-Davies, Phys. Rep. **298**, 81 (1998).

[18] V. M. Pérez-García, H. Michinel, and H. Herrero, Phys. Rev. A **57**, 3837 (1998); L. Salasnich, A. Parola, and L. Reatto, *ibid.* **65**, 043614 (2002).

[19] A. Görlitz *et al.*, Phys. Rev. Lett. **87**, 130402 (2001).

[20] Yu. S. Kivshar and X. Yang, Phys. Rev. E **49**, 1657 (1994).

[21] T. R. Taha and M. J. Ablowitz, J. Comput. Phys. **55**, 203 (1984).

[22] V. E. Zakharov and A. B. Shabat, Zh. Éksp. Teor. Fiz. **64**, 1627 (1973) [Sov. Phys. JETP **37**, 823 (1973)].